RAPID COMMUNICATION

Vortex and anti-vortex compositions of exact elegant Laguerre–Gaussian vector beams

W. Nasalski

Abstract Reformulation of conventional beam definitions into their bidirectional versions and use of Hertz potentials make beam fields exact vector solutions to Maxwell's equations. This procedure is applied to higher-order elegant Laguerre–Gaussian beams of transverse magnetic and transverse electric polarization. Their vortex and anti-vortex co-axial compositions of equal and opposite topological charges are given in a closed analytic form. Polarization components of the composed beams are specified by their radial and azimuthal indices. The longitudinal components are common for beam compositions of both types; meanwhile, their transverse components are different and comprise two—nonparaxial and paraxial—separate parts distinguished by a paraxial parameter and its inverse, respectively. The new solutions may appear useful in modeling and tailoring of arbitrary vector beams.

1 Introduction

Light beams can transport angular momentum (AM) along their propagation direction [1]. In general, AM of vector beams is composed of two parts—spin angular momentum (SAM) and orbital angular momentum (OAM). SAM is associated with beam circular polarization, and OAM is associated with phase profiles of beam fields. For propagation in free space and homogeneous beam polarization, both parts of AM are independent of each other and separately conserved [2]. However, in other cases, SAM and OAM are in general interrelated and can be even inter-converted. The phenomena of the SAM–OAM coupling or their spin-to-orbital conversion are not only interesting by themselves but may be used in many photonic applications [3]. For these reasons, spatial structures of vector beams are recently under intense study. In particular, complex structures of paraxial vector Laguerre–Gaussian (LG) beams and their superpositions were analyzed and inter-relations between their polarization and field vortex structures were indicated [4–8]. However, for beams of transverse diameters close to a wavelength or for pulses of duration close to one cycle, paraxial description of them is no longer adequate and exact beam representations governed by a full set of Maxwell's equations should be implemented instead. Several inventions were already published within this range, mainly for localized wave solutions of fundamental mode, cf. references in [9]. In this letter, exact wave packet solutions built from the LG functions were recently proposed. Their specification to exact beam solutions is described in this work.

The approach presented in this work consists of three subsequent steps. In the first step, time and a spatial coordinate along a beam propagation direction are treated on equal footing. That results in a bidirectional representation of beam fields, where the beam envelopes depend not only on spatial coordinates but also on time. This technique, known in electromagnetics and optics for a long time [10, 11], has been extensively used in construction, for example, focus modes and localized wave packets [12–14]. Next, a scalar solution to the propagation problem is stipulated in the modified form of the elegant (complex argument) Laguerre–Gaussian (eLG) beams known from their paraxial version [15, 16]. Basic definitions and characteristic features of such beams were also presented in [17] in the context of their cross-polarized interactions with dielectric interfaces.

W. Nasalski (✉)
Institute of Fundamental Technological Research,
Polish Academy of Sciences, Adolfa Pawińskiego 5b,
02-106 Warsaw, Poland
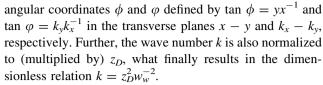e-mail: wnasal@ippt.pan.pl

However, because of the different definitions of the beam envelope and the field propagation factors introduced in the first step, the scalar eLG beam fields are now exact, not paraxial, as they obey exactly the wave equation. In the final step, a full vector representation of the beam field is given in terms of Hertz vector potentials [10]. Transverse magnetic (TM) and electric (TE) exact solutions to Maxwell's equations can be then readily obtained and further superposed into a form of new solutions.

There are two main characteristic features of the new solutions obtained. The first one is the systematic use of higher-order eLG beams in the construction of the bidirectional vector solutions. The eLG beams are well-behaved physical entities. They constitute a complete and bi-orthogonal base for square integrated functions and carry finite energy, linear and angular momenta per unit length along their propagation direction. They can always be given in a closed form in both configuration and spectral domains. Thus, no approximations or expansions are necessary in this approach. The field is given explicitly in an analytic form with beam spatial shape determined by indices of the eLG functions and a beam cross-section diameter. The second characteristic feature of this analysis is the explicit separation of exact beam fields into two ingredients recognized as nonparaxial and paraxial parts of exact solutions. They are also exact scalar solutions to the wave equation by themselves and are distinguished by factors expressed by a paraxial parameter and its inverse, respectively. This field separation can be accomplished by appropriate scaling of spatial and spectral coordinates in the beam field representations. Hence, in all expressions, except these in Eqs. (12) and (13), in which the propagation direction is not specified, spatial coordinates are in normalized, dimensionless form.

The transverse coordinates x and y are normalized to (divided by) a transverse scale w_w of the meaning of a Gaussian beam radius at its waist. The longitudinal (along the propagation direction) coordinate z and $\tau = ct$, as well as the phase front curvature radius R, are normalized to (divided by) $z_D = kw_w^2$ of the meaning of a beam diffraction or Rayleigh length; k, c, and t are a wave number, phase velocity, and time, respectively. The ratio of both scales determines a beam paraxiality level $f = 2^{-1/2}z_D^{-1}w_w$. Similarly, in the spectral domain, the transverse, k_x and k_y, coordinates are normalized to (multiplied by) w_w. The same normalization is also applied to the alternative, longitudinal (real), and transverse (complex) coordinates, respectively, [9]:

$$z_\pm = z \pm \tau, \quad \varsigma_\pm = \frac{1}{\sqrt{2}}(x \pm iy), \quad \kappa_\pm = \frac{1}{\sqrt{2}}(k_x \pm ik_y). \tag{1}$$

Equivalent expressions $\varsigma_\pm = \varsigma_\perp \exp(\pm i\phi)$ and $\kappa_\pm = \kappa_\perp \exp(\pm i\varphi)$ for the transverse coordinates relate them to the angular coordinates ϕ and φ defined by $\tan \phi = yx^{-1}$ and $\tan \varphi = k_y k_x^{-1}$ in the transverse planes $x - y$ and $k_x - k_y$, respectively. Further, the wave number k is also normalized to (multiplied by) z_D, what finally results in the dimensionless relation $k = z_D^2 w_w^{-2}$.

The beams considered here propagate in free space. They are of cylindrical symmetry in intensity, with their beam axes along the z-axis and their waists placed at a transverse plane $z = 0$. Their electric and magnetic fields are normalized to (multiplied by) by square roots of the free space admittance and impedance, respectively. Scalar and vector versions of the exact eLG beams of arbitrary order will be analyzed in Sects. 2 and 3, respectively. Vortex and anti-vortex superpositions of two overlapping and co-propagating eLG beams will be presented in Sects. 4 and 5, respectively. The analysis will be shortly concluded in Sect. 6.

2 Exact scalar eLG beams

Let us start from the scalar field g' obeying the wave equation in free space:

$$\left[2(w_w/z_D)^2 \partial_{z_+} \partial_{z_-} + \partial_{\varsigma_+} \partial_{\varsigma_-}\right] g'(\varsigma_+, \varsigma_-, z_+, z_-) = 0. \tag{2}$$

The function g', given for the specified wave number k, depends on both longitudinal coordinates $z_\pm$. If g' is factorized into the envelope g dependent on z_+ and the propagation factor dependent on z_-; $g' = g \exp(ikz_-)$, then the wave equation reduces exactly to the paraxial equation with its fundamental Gaussian solution g [9]:

$$\left(2i\partial_{z_+} + \partial_{\varsigma_+} \partial_{\varsigma_-}\right)g(\varsigma_+, \varsigma_-, z_+) = 0, \tag{3}$$

$$g(\varsigma_+, \varsigma_-, z_+) = v^{-2}(z_+) \exp\left[-\varsigma_+\varsigma_- v^{-2}(z_+)\right]. \tag{4}$$

The beam complex radius v specifies the real beam parameters: the beam width diameter $2w$ and the radius R of phase front curvature; $v^2 = 1 + i2^{-1}z_+ = (w^{-2} - iR^{-1})^{-1}$. On the other hand, the paraxial Eq. (3) describes also the conventional Gaussian envelope $\breve{g}$ after the replacement of z_+ by $2z$, as its complex width squared $\breve{v}^2 = 1 + iz$ depends only on z.

Higher-order eLG solutions $G_{p,\pm l}$ to (3) are obtained by the appropriate differentiation of $g \equiv G_{0,0}$ [17]. That separates vortex factors in the beam definition, $G_{p,\pm l} = Q_{p,l} \exp(\pm il\phi)$, where

$$G_{p,\pm l}(\varsigma_+, \varsigma_-, z_+) = \partial_{\varsigma_\pm}^p \partial_{\varsigma_\mp}^{p+l} g(\varsigma_+, \varsigma_-, z_+), \tag{5}$$

$$Q_{p,l}(\varsigma_+, \varsigma_-, z_+) = (-1)^{p+l} p! v^{-(2p+l)} u^l L_p^l(u^2) g(\varsigma_+, \varsigma_-, z_+), \tag{6}$$

$u^2 = \varsigma_+\varsigma_- v^{-2}$, $l = |l|$ and $Q_{0,0} = g$. The function $Q_{p,l}$ and the associated Laguerre polynomials L_p^l are specified by the

nonnegative radial and azimuthal indices p and l and are independent of φ and the sign of $\pm l$. The signs $\pm$ refer to opposite helicities presented by the vortex factors in the eLG solutions. Note that the conventional paraxial eLG beams $\breve{G}_{p,\pm l}$ are also defined by (5) and (6) with the single replacement z_+ by $2z$.

The Fourier transform of Weyl type [10] yields the definitions (5) and (6) restated in the spectral domain [17]:

$$G_{p,\pm l}(\varsigma_+, \varsigma_-, z_+) = \frac{i}{2\pi} \int d\kappa_+ d\kappa_- \tilde{G}_{p,\pm l}(\kappa_+, \kappa_-, z_+) e^{i(\kappa_+ \varsigma_- + \kappa_- \varsigma_+)}. \tag{7}$$

$$\tilde{G}_{p,\pm l}(\kappa_+, \kappa_-, z_+) = i^{2p+l} \kappa_{\mp}^{p} \kappa_{\pm}^{p+l} \tilde{g}(\kappa_+, \kappa_-, z_+), \tag{8}$$

$$\tilde{Q}_{p,l}(\kappa_+, \kappa_-, z_+) = (-\kappa_+ \kappa_-)^{p+l/2} \tilde{g}(\kappa_+, \kappa_-, z_+), \tag{9}$$

where $\tilde{G}_{p,\pm l} = \tilde{Q}_{p,l} \exp(\pm il\varphi)$ and $\tilde{g} = exp(-\kappa_+ \kappa_- v^2)$. The definition (8) allows also for alternative representations of the eLG functions in the spectral domain:

$$\tilde{G}_{p,\pm l} = \tilde{G}_{p+1/2, \pm(l-1)} e^{\pm i\varphi} = \tilde{G}_{p+1, \pm(l-2)} e^{\pm 2i\varphi}, \tag{10}$$

$$\tilde{G}_{p,\pm l} = \tilde{G}_{p-1/2, \pm(l+1)} e^{\mp i\varphi} = \tilde{G}_{p-1, \pm(l+2)} e^{\mp 2i\varphi}, \tag{11}$$

and, in parallel, for $G_{p,\pm l}$ in the configuration domain [9], all interrelated by the transform (7).

In both, scalar and vector, beam solutions, their radii v, w, and R depend on z_+ and in turn z_+ depends on both, longitudinal and time, spatial coordinates z and $\tau = ct$. Therefore, the eLG beams $G_{p,\pm l}$ differ in general from the conventional paraxial eLG beams $\breve{G}_{p,\pm l}$ dependent on z instead of z_+. However, at the initial time $t = 0$, $z_+ = z = z_-$ and the beams copy their conventional counterparts, although with its coordinate z shortened twice. Moreover, at the phase front plane and for any time moment, $z = ct$ or $z_- = 0$ and $z_+ = 2z$. In this case, the beam field distribution remains exactly in the conventional form with the following shifts along the z-axis: its waist position (at $z_+ = 0$) is shifted by $-z$, together with its on-axis phase shifted by $-2kz$. Similar relations for the beam on-axis phase shift and waist position can be found for arbitrary values of t and z. Thus, the exact eLG beams are physical entities to the same extent as the conventional paraxial eLG beams are.

3 Exact vector eLG beams

Exact solutions to Maxwell's equations can be built from the Hertz vector potentials $\boldsymbol{M}'$ and $\boldsymbol{N}'$ [10]. For symmetry reasons, both of them are taken directed along the beam axis, that is, they possess only one nonzero component M'_z and N'_z, respectively. The total field can be then decomposed of the two collinear and orthogonal TM and TE solutions:

$$\boldsymbol{E}' = \boldsymbol{E}'^{(tm)} + \boldsymbol{E}'^{(te)} = \nabla \times \nabla \times \boldsymbol{M}' - \partial_\tau \nabla \times \boldsymbol{N}', \tag{12}$$

$$\boldsymbol{H}' = \boldsymbol{H}'^{(tm)} + \boldsymbol{H}'^{(te)} = \nabla \times \nabla \times \boldsymbol{N}' + \partial_\tau \nabla \times \boldsymbol{M}', \tag{13}$$

where, exceptionally, the coordinates x, y, z, and t are not normalized. In the cylindrical circular polarization frame $(\hat{\boldsymbol{e}}_R, \hat{\boldsymbol{e}}_L, \hat{\boldsymbol{e}}_z)$ and with scalar potentials $M'_z = M'w_w^2$ and $N'_z = N'w_w^2$, Eqs. (12) and (13) yield [9]:

$$\boldsymbol{E}'^{(tm)} = -2\hat{\boldsymbol{e}}_z \partial_{\varsigma_+} \partial_{\varsigma_-} \boldsymbol{M}' + (w_w/z_D)(\hat{\boldsymbol{e}}_R \partial_{\varsigma_+} + \hat{\boldsymbol{e}}_L \partial_{\varsigma_-}) \partial_z \boldsymbol{M}', \tag{14}$$

$$\boldsymbol{E}'^{(te)} = i(w_w/z_D)(\hat{\boldsymbol{e}}_R \partial_{\varsigma_+} - \hat{\boldsymbol{e}}_L \partial_{\varsigma_-}) \partial_\tau \boldsymbol{N}', \tag{15}$$

with $\partial_z = \partial_{z+} + \partial_{z-}$ and $\partial_\tau = \partial_{z+} - \partial_{z-}$. The TM and TE solutions are in general independent. If, however, $N'_z = \pm M'_z$, then by duality $\boldsymbol{H}'^{(tm)} = \pm \boldsymbol{E}'^{(te)}$ and $\boldsymbol{H}'^{(te)} = \mp \boldsymbol{E}'^{(tm)}$.

Let the Hertz scalars M' and N' and the field vectors $\boldsymbol{E}'^{(tm)}$ and $\boldsymbol{E}'^{(te)}$ be represented by the envelope factors M, N, $\boldsymbol{E}^{(tm)}$, and $\boldsymbol{E}^{(te)}$ dependent on z_+ and the common propagation factor $\exp(ikz_-)$ dependent on z_-. Consider first the case of equal scalar Hertz potentials expressed by the eLG function $N = M = w_w^2 G_{p,\pm l}$ and convert (14) and (15) from the frame $(\hat{\boldsymbol{e}}_R, \hat{\boldsymbol{e}}_L, \hat{\boldsymbol{e}}_z)$ to the cylindrical polar (radial/azimuthal) frame $(\hat{\boldsymbol{e}}_\rho, \hat{\boldsymbol{e}}_\phi, \hat{\boldsymbol{e}}_z)$:

$$\hat{\boldsymbol{e}}_\rho = 2^{-1/2}(\hat{\boldsymbol{e}}'_R + \hat{\boldsymbol{e}}'_L), \quad i\hat{\boldsymbol{e}}_\phi = 2^{-1/2}(\hat{\boldsymbol{e}}'_R - \hat{\boldsymbol{e}}'_L), \tag{16}$$

$$\hat{\boldsymbol{e}}'_R = \hat{\boldsymbol{e}}_R e^{-i\phi}, \quad \hat{\boldsymbol{e}}'_L = \hat{\boldsymbol{e}}_L e^{+i\phi}. \tag{17}$$

Equation (17) defines the new polarization frame $(\hat{\boldsymbol{e}}'_R, \hat{\boldsymbol{e}}'_L, \hat{\boldsymbol{e}}_z)$ called here as a cylindrical circular hybrid frame. Transverse components of this frame are of zero AM as their SAM is canceled by their vortex factors of opposite OAM. Now, Eqs. (14), (15), (16), and (17), together with the definitions of the paraxial Eq. (3) and the scalar eLG beams (4) and (6), yield four solutions, namely the TM and TE solutions in two cases of opposed chirality, with transverse components of radial and azimuthal polarization, respectively:

$$\boldsymbol{E}_{p,\pm l}^{(tm)} = -2\hat{\boldsymbol{e}}_z Q_{p+1,l} e^{\pm il\phi} + i\hat{\boldsymbol{e}}_\rho (f^{-1} Q_{p,l+1} + f^{+1} Q_{p+1,l+1}) e^{\pm il\phi}, \tag{18}$$

$$\boldsymbol{E}_{p,\pm l}^{(te)} = \hat{\boldsymbol{e}}_\phi (f^{-1} Q_{p,l+1} - f^{+1} Q_{p+1,l+1}) e^{\pm il\phi}, \tag{19}$$

On the grounds of the identities (10) and (11) and the duality principle, Eqs. (18) and (19) are equivalent to Eqs. (6), (7), (9), and (10) in Ref. [9].

The representation (18) and (19) shows quite regular field structure—for the separate paraxial and nonparaxial parts, the field spatial distribution appears of the same

form for both transverse polarization components. The parameter f indicates what part of the solution prevails for paraxial ($f \ll 1$) or nonparaxial ($f \gg 1$) values of the ratio of the beam waist radius to the field wavelength. The paraxial, longitudinal, and nonparaxial contributions to the total field possess the same vortex factor $\exp(\pm il\phi)$ specified by the azimuthal index l. Note that the paraxial and nonparaxial field ingredients in (18) and (19) satisfy exactly the paraxial Eq. (3); meanwhile, the field polarization components in (14) and (15) satisfy exactly the wave Eq. (2).

4 Vortex composition of two co-axial vector eLG beams

For vortex compositions, the scalar Hertz potentials in (14) and (15) are equal; $N = M$. In the hybrid polarization frame $(\hat{e}'_R, \hat{e}'_L, \hat{e}_z)$, cf. (17), the coherent superpositions with relative phase $\mp \pi/2$ of the TM and TE vector eLG beams (18) and (19) of same p and $\pm l$ indices result in two new vector structures $\boldsymbol{E}^{(a)}_{p,\pm l} = 2^{-1/2}\left(\boldsymbol{E}^{(tm)}_{p,\pm l} - i\boldsymbol{E}^{(te)}_{p,\pm l}\right)$ and $\boldsymbol{E}^{(b)}_{p,\pm l} = 2^{-1/2}\left(\boldsymbol{E}^{(tm)}_{p,\pm l} + i\boldsymbol{E}^{(te)}_{p,\pm l}\right)$ of vortex beams:

$$\boldsymbol{E}^{(a)}_{p,\pm l} = \boldsymbol{E}^{(a)}_{\perp;p,\pm l} - 2^{1/2}\hat{e}_z Q_{p+1,l}e^{\pm il\phi}, \tag{20}$$

$$\boldsymbol{E}^{(b)}_{p,\pm l} = \boldsymbol{E}^{(b)}_{\perp;p,\pm l} - 2^{1/2}\hat{e}_z Q_{p+1,l}e^{\pm il\phi}, \tag{21}$$

$$\boldsymbol{E}^{(a)}_{\perp;p,\pm l} = i\left(\hat{e}'_L f^{-1}Q_{p,l+1} + \hat{e}'_R f^{+1}Q_{p+1,l+1}\right)e^{\pm il\phi}, \tag{22}$$

$$\boldsymbol{E}^{(b)}_{\perp;p,\pm l} = i\left(\hat{e}'_R f^{-1}Q_{p,l+1} + \hat{e}'_L f^{+1}Q_{p+1,l+1}\right)e^{\pm il\phi}, \tag{23}$$

with the transverse field components labeled by the subscript $\perp$. In each case (a) and (b), there are two independent solutions differentiated by the sign of $\pm l$. The field structure is now even more regular than that one in the cylindrical polar polarization frame. For the separate—paraxial, longitudinal, and nonparaxial—field contributions, the exact field spatial structures (a) and (b) appear of the same spatial form in four solutions given in (20), (21), (22) and (23). The transverse beam components (22) and (23) show symmetry with respect to the beam polarization; $\boldsymbol{E}^{(a)}_{p,\pm l}$ can be obtained from $\boldsymbol{E}^{(b)}_{p,\pm l}$, and vice versa, by the simple replacement $\hat{e}'_R \leftrightarrow \hat{e}'_L$. The amplitude ratio between the nonparaxial and paraxial parts of the field is always related by the ratio $(f/v)^2(p+1)L^l_{p+1}\big/L^l_p$ dependent on z_+. For all the polarization field components, OAM amounts $\pm l\hbar$ per photon [1, 2]. In spite of the use of elegant rather than standard LG beams, the paraxial parts of the solution (20), (21), (22) and (23) correspond to the compositions of the paraxial solutions (I)–(IV) presented in [8] for standard LG beams.

5 Anti-vortex composition of two co-axial vector eLG beams

In the case of anti-vortex compositions, the scalar Hertz potentials in (14) and (15) are of opposite azimuthal indices and take on the form $M = G_{p,\pm l}$ and $N = G_{p,\mp l}$. The TM solutions in (18) remain the same but the TE solutions (19) now possess vortex factors of opposite helicity:

$$\boldsymbol{E}^{(te)}_{p,\mp l} = \boldsymbol{E}^{(te)}_{p,\pm l}\exp(\mp 2il\phi). \tag{24}$$

Then, the composition beam fields $\boldsymbol{E}^{(c)}_{p,\pm l} = 2^{-1/2}\left(\boldsymbol{E}^{(tm)}_{p,\pm l} - i\boldsymbol{E}^{(te)}_{p,\mp l}\right)$ and $\boldsymbol{E}^{(d)}_{p,\pm l} = 2^{-1/2}\left(\boldsymbol{E}^{(tm)}_{p,\pm l} + i\boldsymbol{E}^{(te)}_{p,\mp l}\right)$ equal the $\mp\pi/2$ phase shifted superposition of these solutions:

$$\boldsymbol{E}^{(c)}_{p,\pm l} = \boldsymbol{E}^{(c)}_{\perp;p,\pm l} - 2^{1/2}\hat{e}_z Q_{p+1,l}e^{\pm il\phi}, \tag{25}$$

$$\boldsymbol{E}^{(d)}_{p,\pm l} = \boldsymbol{E}^{(d)}_{\perp;p,\pm l} - 2^{1/2}\hat{e}_z Q_{p+1,l}e^{\pm il\phi}, \tag{26}$$

$$\boldsymbol{E}^{(c)}_{\perp;p,\pm l} = \hat{e}'_L\left[if^{-1}\cos(l\phi)Q_{p,l+1} \mp f^{+1}\sin(l\phi)Q_{p+1,l+1}\right] \\ \mp \hat{e}'_R\left[f^{-1}\sin(l\phi)Q_{p,l+1} \mp if^{+1}\cos(l\phi)Q_{p+1,l+1}\right], \tag{27}$$

$$\boldsymbol{E}^{(d)}_{\perp;p,\pm l} = \hat{e}'_R\left[if^{-1}\cos(l\phi)Q_{p,l+1} \mp f^{+1}\sin(l\phi)Q_{p+1,l+1}\right] \\ \mp \hat{e}'_L\left[f^{-1}\sin(l\phi)Q_{p,l+1} \mp if^{+1}\cos(l\phi)Q_{p+1,l+1}\right]. \tag{28}$$

The symmetries $\hat{e}'_R \leftrightarrow \hat{e}'_L$ between $\boldsymbol{E}^{(c)}_{\perp;p,\pm l}$ and $\boldsymbol{E}^{(d)}_{\perp;p,\pm l}$ are similar to those for the vortex composition but in (27) and (28), the trigonometric functions replace the corresponding exponent functions in (22) and (23) separately for the paraxial and nonparaxial parts of the solution. The previous amplitude ratio between these transverse parts is now additionally multiplied by $\mp i\cot(l\phi)$ and $\pm i\tan(l\phi)$ for the right-handed and left-handed hybrid polarization components of $\boldsymbol{E}^{(c)}_{\perp;p,\pm l}$, respectively, and vice versa for $\boldsymbol{E}^{(d)}_{\perp;p,\pm l}$. This ratio depends now not only on z_+ but also on ϕ, and the intensity patterns of the anti-vortex compositions comprise $2l$ petals placed in opposed angular positions for the paraxial and nonparaxial parts. In centers of these petals, the transverse field is in pure hybrid states $\hat{e}'_R$ or $\hat{e}'_L$. Total OAM disappears for the transverse beam components; meanwhile, for the longitudinal components, it is still equal $\pm l\hbar$ per photon. For the paraxial part of the solution (27) and (28), correspondence can also be found with results presented in [6] for standard LG beams.

6 Conclusions

In general, the beam field compositions can be obtained by arbitrary superposition of TM and TE solutions $\alpha\boldsymbol{E}^{(tm)}_{p,\pm l} +$

$\beta \boldsymbol{E}_{p,l'}^{(te)}$ with complex numbers α and β, where $l' = \pm l$ and $l' = \mp l$ for the vortex and anti-vortex compositions, respectively. In Sect. 4, the solutions were given for $\beta = \pm i\alpha$. Other composition solutions, like these for $\beta = \pm \alpha$, can be derived per analogy. There are also other choices in construction vector eLG beams by using, for example, transverse instead of longitudinal vector potentials or collinear eLG beams of different amplitudes and/or with different vortex charges. However, the vortex and anti-vortex beam compositions are built here from the equal in magnitude longitudinal Hertz potentials. Their characteristics seem to be particularly useful for interpretation of more complex field structures of beams.

Transverse components of these solutions are defined in the nonuniform orthogonal polarization hybrid frame $(\hat{\boldsymbol{e}}_R', \hat{\boldsymbol{e}}_L')$ and composed of two—nonparaxial and paraxial—parts, which are always associated with the paraxial parameter and its inverse, respectively. On the contrary, the longitudinal part, common for both compositions, does not depend on this parameter. Each of these beam parts, with the propagation factor included, satisfies the wave equation separately and is specified differently by their radial and azimuthal indices. Although the circular frame $(\hat{\boldsymbol{e}}_R, \hat{\boldsymbol{e}}_L)$ is convenient in field derivations and the orthogonal solutions are separated in the polar frame $(\hat{\boldsymbol{e}}_\rho, \hat{\boldsymbol{e}}_\phi)$, the hybrid frame $(\hat{\boldsymbol{e}}_R', \hat{\boldsymbol{e}}_L')$ appears more suitable for description of the beam compositions.

It should be finally noted that the beams considered here may be regarded of forward propagation monochromatic type, as obtained for one specified value of the wave number k. However, the beam fields depend on z_- only through their propagation factors; meanwhile, the field envelopes depend on z_+ through the beam complex width v. Still, after the replacement $z_\pm \to z_\mp$ and appropriate redefinition of v in all above expressions, the results presented remain valid also for backward propagation case. Therefore, the field compositions of counterpropagating beams are then readily available by analogy. In general, series consisted of the solutions of both these types, with different radial and azimuthal indices and polarization, should yield beam fields determined by arbitrary initial conditions specified at any plane transverse to the beam propagation direction.

References

1. L. Allen, S.M. Barnett, M.J. Padgett, *Orbital Angular Momentum* (Institute of Optics Publishing, 2003)
2. S.M. Barnett, Optical angular-momentum flux. J. Opt. B: Quantum Semiclass. Opt. **4**, S7–S15 (2002)
3. L. Marrucci, E. Karimi, S. Slussarenko, B. Piccirillo, E. Santamato, E. Nagali, F. Sciarrino, Spin-to-orbital conversion of the angular momentum of light and its classical and quantum applications. J. Opt. **13**, 064001-1–064001-13 (2011)
4. M.A.A. Neil, T. Wilson, T. Juškaitis, A wavefront generator for complex pupil function synthesis and point spread function engineering. J. Microcopy **197**, 219–223 (2000)
5. C. Maurer, A. Jesacher, S. Fürhapter, S. Bernet, M. Ritsch-Marte, Tailoring of arbitrary optical vector beams. New J. Phys. **9**, 78-1–78-20 (2007)
6. S. Franke-Arnold, J. Leach, M.J. Padgett, V.E. Lembessis, D. Ellinas, A.J. Wright, J.M. Girkin, P. Öhberg, A.S. Arnold, Optical ferris wheel for ultracold atoms. Opt. Express **15**, 8619–8625 (2007)
7. T. Ando, N. Matsumoto, Y. Ohtake, Y. Takiguchi, T. Inoue, Structure of optical singularities in coaxial superpositions of Laguerre–Gaussian modes. J. Opt. Soc. Am. A **27**, 2602–2612 (2010)
8. S. Vyas, Y. Kozawa, S. Sato, Polarization singularities in superposition of vector beams. Opt. Express **21**, 8972–8986 (2013)
9. W. Nasalski, Exact elegant Laguerre–Gaussian vector wave packets. Opt. Lett. **38**, 809–811 (2013)
10. J.A. Stratton, *Electromagnetic theory* (McGraw-Hill, New York, 1941)
11. H. Bacry, M. Cadilhac, Metaplectic group and Fourier optics. Phys. Rev. A **23**, 2533–2536 (1981)
12. R.W. Ziolkowski, Exact solutions of the wave equation with complex source locations. J. Math. Phys. **26**, 861–863 (1985)
13. A. Sezginer, A general formulation of focus wave modes. J. Appl. Phys. **57**, 678–683 (1985)
14. P. Hillion, Spinor focus wave modes. J. Math. Phys. **28**, 1743–1748 (1987)
15. T. Takenaka, M. Yokota, O. Fukumitsu, Propagation of light beams beyond the paraxial approximation. J. Opt. Soc. Am. A **2**, 826–829 (1985)
16. E. Siegman, *Lasers* (University Science, Mill Valley, 1986)
17. W. Nasalski, Polarization versus spatial characteristics of optical beams at a planar isotropic interface. Phys. Rev. E **74**, 056613-1-16 (2006)